

AD-A273 698



SEMIANNUAL TECHNICAL REPORT

1 JAN 93 to 31 JUN 93

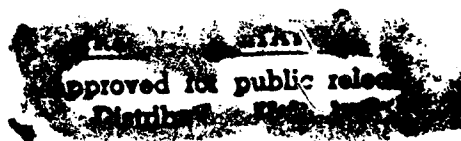
The In Situ Observation of Epitaxial Diamond Thin Film Nucleation
and Growth Using Emission Electron Microscopy

Submitted by

Martin E. Kordesch
Associate Professor of Physics
Ohio University, Athens, Ohio
Tel.: (614) 593 - 1703, FAX: - 0433
electronic mail: kordesch@helios.phy.ohiou.edu

Grant No. N00014-91-J-1596
R&T Number: s400028ssr02

DTIC
ELECTE
DEC 15 1993
S E D



93-30315



4006

93 12 14 049

**Best
Available
Copy**

REPORT DOCUMENTATION PAGE			Form Approved OMB No. 0704-0188	
Public reporting burden for this collection of information is estimated to average 1 hour per response, including the time for reviewing instructions, searching existing data sources, gathering and maintaining the data needed, and completing and reviewing the collection of information. Send comments regarding this burden estimate or any other aspect of this collection of information, including suggestions for reducing this burden, to Washington Headquarters Services, Directorate for Information Operations and Reports, 1215 Jefferson Davis Highway, Suite 1204, Arlington, VA 22202-4302, and to the Office of Management and Budget, Paperwork Reduction Project (0704-0188), Washington, DC 20503.				
1. AGENCY USE ONLY (Leave blank)	2. REPORT DATE DEC - 93	3. REPORT TYPE AND DATES COVERED Semiannual 1-JAN-93 to 30-JUN-93		
4. TITLE AND SUBTITLE The In Situ Observation of Epitaxial Diamond Thin Film Nucleation and Growth using Emission Electron Microscopy		5. FUNDING NUMBERS G: N00014-91-J-1596		
6. AUTHOR(S) Martin E. Kordesch				
7. PERFORMING ORGANIZATION NAME(S) AND ADDRESS(ES) Ohio University Department of Physics and Astronomy Athens, Ohio 45701-2979 Claire Carlson, Administrative Contact		8. PERFORMING ORGANIZATION REPORT NUMBER		
9. SPONSORING/MONITORING AGENCY NAME(S) AND ADDRESS(ES) Max N. Yoder, ONR - 314 Office of Naval Research 800 N. Quincy St. Arlington, VA 22217-5660		10. SPONSORING/MONITORING AGENCY REPORT NUMBER		
11. SUPPLEMENTARY NOTES				
12a. DISTRIBUTION / AVAILABILITY STATEMENT Approved for Public Release, distribution unlimited			12b. DISTRIBUTION CODE	
13. ABSTRACT (Maximum 200 words) In situ observation of CVD diamond dissolution and etching using photoemission electron microscopy (PEEM) suggests that nucleation of diamond occurs directly on Mo, with a Mo-carbide bulk diffusion barrier that facilitates surface carbon transport for growth. Low energy electron microscopy of doped homoepitaxial C(100) is hindered by surface roughness, which is visible in PEEM. Charging observed with type IIa diamond is no longer present, but the high secondary electron yield is still problematic for direct imaging. TEM studies of CVD diamond grown directly on Mo TEM grids show a 10nm thick amorphous C layer after growth, which is easily removable with an isopropanol rinse. LEED studies of Si(310) substrates for diamond growth show a (2X1) Si(310) reconstructed surface, with some faceting with four-fold symmetry. Nucleation is sparse and random on the Si(310) surfaces examined to date.				
14. SUBJECT TERMS CVD Diamond, Nucleation, emission microscopy, in situ electron microscopy, STM, Si(310)			15. NUMBER OF PAGES 40	
			16. PRICE CODE	
17. SECURITY CLASSIFICATION OF REPORT unclassified	18. SECURITY CLASSIFICATION OF THIS PAGE unclassified	19. SECURITY CLASSIFICATION OF ABSTRACT unclassified	20. LIMITATION OF ABSTRACT UL	

CONTENTS

page

Contents.....3

1.0 Summary of Progress

- 1.1 In situ Observation of Diamond Nucleation and Growth...4
 - 1.11 PEEM studies of CVD Diamond on Mo.....4
 - 1.12 TEM studies of non diamond carbon on diamond....4
 - 1.13 Re-growth and diamond dissolution on Mo.....5
- 1.2 Preparation of stepped/faceted Si(310) surfaces.....5
 - Figures 1 and 26
- 1.3 Lateral Carbon Layer Growth on Mo(100).....7
- 1.4 LEEM observation of the C(100)-H surface.....7
- 1.5 Emission Microscopy observation of the segregation of carbon to the surface of Copper.....7

2.0 Publications/Presentations.....8

3.0 Appendix (referenced papers).....9

Accession For	
NTIS CRA&I	<input checked="" type="checkbox"/>
DTIC TAB	<input type="checkbox"/>
Unannounced	<input type="checkbox"/>
Justification	
By	
Distribution /	
Availability Codes	
Dist	Avail and/or Special
A-1	

DTIC QUALITY INSPECTED 1

Summary of Progress:

Experimental efforts are concentrated on (1) showing that conditions in our in situ growth system are sufficient for diamond growth, (2) the preparation of substrates with high step-terrace density that are suitable templates for diamond heteroepitaxy and (3) development of a two-dimensional diamond growth method.

Progress toward these three objectives is described below.

1.1 In situ Observation of Diamond Nucleation and Growth

The examination of CVD diamond grown for short times on Mo substrates with varying pre-treatments has been examined and presented in a Ph.D. dissertation (see publications). Several conclusions were drawn from the work: (1) on Mo substrates, the formation of Mo-carbide acted as a nucleation inhibitor, (2) diamond seeds, remaining after polishing the substrate, could be removed by suitable heat treatment, which was found to be a combination of the temperature and the heating time.

1.11 PEEM studies of CVD Diamond on Mo

Further examination of the substrate morphology also indicated that Mo-carbide was a diffusion barrier to both carbon and Mo transport through the growth interface. In particular, diamond was stable while in contact with Mo-carbide, while a Mo-C or Mo-diamond interface was reactive until a sufficient carbide diffusion barrier was formed. A final, practical result was the observation that a diamond seeded Mo-carbide surface was an ideal growth surface, with high nucleation density, since seeds survived on top of the barrier Mo-carbide layer. A summary of the work is presented in the Diamond and Related Materials (Wang, et al.) paper cited in the Appendix.

The question of the practicality of in situ observation of diamond nucleation at pressures below 1×10^{-3} Torr hydrogen/methane has not been answered. A new initiative, the use of supersonic molecular beams to grow diamond, is in the planning stage. The local reactant pressures will be increased by up to 4 orders of magnitude over present concentrations. Success with this method may solve the nucleation observation problem, by increasing the reactant pressures to those commonly used in CVD reactors.

1.12 TEM studies of non-diamond carbon on diamond

Measurements of CVD diamond grown directly on Mo TEM specimen grids were made through a collaboration with the Fritz Haber Institute in Berlin, Germany. This effort was funded in part by a NATO travel grant. The first results of this

collaboration are presented in a short Letter by Engel, et al., submitted to Diamond and Related Materials, reprinted in the Appendix

1.13 Re-growth and diamond dissolution on Mo

As a continuation of our study of the role of Mo-carbide in CVD diamond nucleation, Mo TEM grids were used for different lengths of time in our hot filament CVD reactor, to create different Mo-carbide substrates for nucleation. Some grids were used for two growth cycles, so that diamond dissolution, and the Mo-carbide diamond attachment site could be studied. These images and diffraction data are currently being examined.

1.2 Preparation of stepped/faceted Si(310) surfaces

An issue central to the growth of defect-free, electronic grade heteroepitaxial growth of CVD diamond is the role of "high energy" sites on the surface, such as steps, which may be equivalent to the "scratches" that are commonly found to nucleate diamond. It may be possible to nucleate diamond at a step, then grow the CVD heteroepitaxial diamond layer laterally across the surface by the "step flow" mechanism. The Si(310) surface may form a stable faceted surface that contains mono-atomic height (100) and (111) faces that could be used for CVD diamond heteroepitaxy. It will be necessary to know if: (1) the stepped surface can be prepared (2) the (310) surface survives CVD growth methods (3) the surface forms a carbide, and what crystal structure this layer has, and (4) does diamond nucleates at the steps that result.

Preliminary results for the preparation of the Si(310) surface indicate that a (100) type facet may be the predominant surface feature. A LEED pattern is shown for a "clean", annealed surface. The LEED pattern has a four-fold symmetry, the Si(310) has only mirror symmetry and possibly a glide plane. The LEED data suggest reconstruction. An STM image of the reconstructed Si(310) surface is also shown. Regular features were not observed. Diamond growth on the Si(310) surface was not oriented relative to the substrate and sparsely nucleated.

The surface structure has not been conclusively identified, and this work continues.

Figure 1.: LEED Pattern of Si(310) surface, probably a reconstructed surface layer. $E = 62$ eV. Artists conception: the four small spots around the larger spots are observed in all cases, but the whole pattern may be centered, and may not have four-fold symmetry.

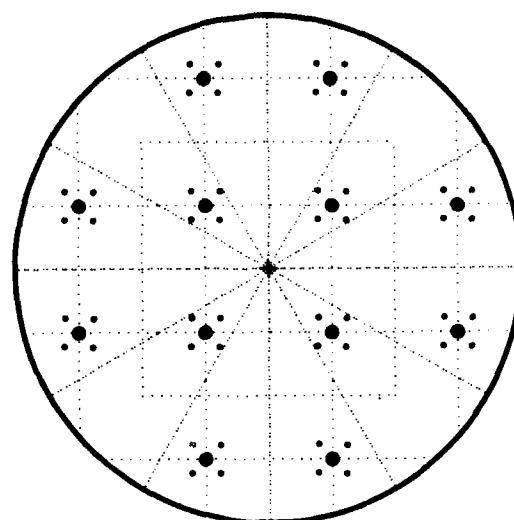
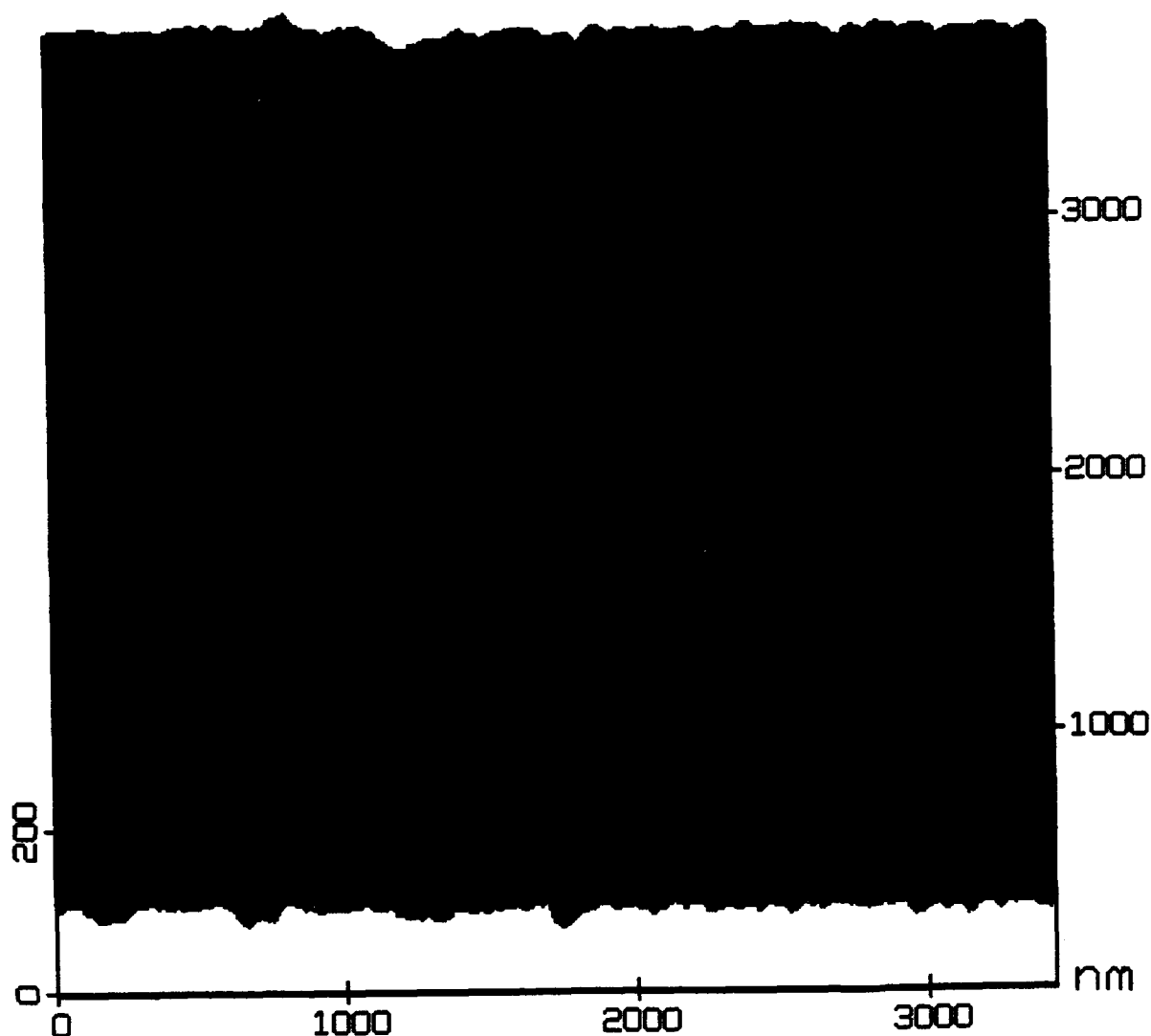


Figure 2.: STM of same Si(310) surface as in Fig. 1. No discernable surface ordering is present.



1.3 Lateral Carbon Layer Growth on Mo(100)

In order to continue our modified ALE (Atomic Layer Epitaxy) approach to diamond heteroepitaxy, a Scanning Auger Microscope was added to our system to analyze the composition of the reaction fronts observed during deposition. Design and installation are proceeding.

1.4 LEEM observation of the C(100)-H surface

The charging of type IIa natural diamond substrates has made LEEM imaging of the surface difficult in our LEEM. We have attempted to obtain a doped, homoepitaxial C(100) crystal with only limited success. We are exploring the possibility of purchasing a suitable naturally semiconducting C(100) crystal for observation.

1.5 Emission Microscopy observation of the segregation of carbon to the surface of Copper

A small emission microscope built to observe in situ the thermal segregation of C to the surface of an ion-implanted Cu specimen has been built. First measurements indicate that the evaporation of Cu occurs at a temperature below the thermionic emission threshold. Proof of principle studies will be conducted with manganese, where this problem is not present. Addition of carbon to the Cu substrate may still preserve the original experimental design. If not, an UV illumination source will be added so that photoemission images may also be obtained.

2.0 Publications:

1. A Photoemission Electron Microscope Investigation of Chemical Vapor Deposition Diamond Films and Diamond Nucleation, Congjun Wang, Ph.D. Dissertation, UMI Dissertation Services, 1993, No. 9322371.
2. Sample Tilting Mechanism and Transfer System for High Temperature Thin Film Deposition and Ultra High Vacuum Photoelectron Microscopy, Adrian Garcia and Martin E. Kordesch, J. Vac. Sci. Technol., 11 (1993) 461-3.
3. Electron Emission Microscopy for In Situ Studies of Diamond Surfaces and CVD Diamond Nucleation and Growth, M.E. Kordesch, Proceedings of the Third International Symposium on Diamond Materials, J.P. Dismukes and K.V. Ravi, eds., The Electrochemical Society, Pennington, NJ, 1993, pg 787.
4. Introduction to Emission Electron Microscopy for the in situ Study of Surfaces, Martin E. Kordesch, Proceedings of the 51st Annual Meeting of the Microscopy Society of America, G.W. Bailey and C.L. Rieder, eds., San Francisco Press, San Francisco, CA 1993.

Appended Papers submitted/ accepted for Publication:

5. Real-time, in situ Photoelectron Emission Microscopy Observation of CVD diamond Oxidation and Dissolution on Molybdenum, C. Wang, J.D. Shovlin, M.E. Kordesch and J.M. MaCauley, Accepted for Diamond and Related Materials.
6. Non-Diamond Carbon Removal from CVD Diamond, W. Engel, D.C. Ingram, J.C. Keay and M.E. Kordesch, submitted to Diamond and Related Materials.

Presentations:

1. "Electron Emission Microscopy for In Situ Studies of Diamond Surfaces and CVD Diamond Nucleation and Growth, M.E. Kordesch, Third International Symposium on Diamond Materials, ECS Hawaii, May 1993.
2. ---, University of Illinois at Chicago, March 1993.
3. ---, Fritz Haber Institute, Berlin, June 1993.

3.0 Appendix:

**Real-Time, In Situ Photoelectron Emission Microscopy
Observation of CVD Diamond Oxidation and Dissolution
on Molybdenum**

Congjun Wang, Joseph D. Shovlin and Martin E. Kordesch

**Condensed Matter and Surface Sciences Program
Department of Physics and Astronomy
Ohio University
Athens, OH 45701-2979**

and

John M. Macaulay

**Silicon Video Corp.
Cupertino CA 95014**

Abstract

The oxidation and dissolution of sparsely nucleated, 1-2 μm diameter hot filament CVD diamonds on polycrystalline molybdenum (Mo) substrates is observed in situ, in real-time using photoelectron emission microscopy (PEEM). At about 875 K, $p_{\text{ox}} = 3 \times 10^{-8}$ Torr, CVD diamond is etched by oxygen, leaving the Mo/Mo-carbide substrate complex unaffected. Dissolution of CVD diamond into the Mo substrate begins at about 1475 K in ultra high vacuum. Oxidative removal of diamond leaves pits in the substrate; diamond dissolution results in raised, bump-like hillocks. These bumps are identified with x-ray photoelectron spectroscopy as Mo-carbide. The substrate morphology after oxygen etching and dissolution indicates that the Mo-carbide is primarily a barrier against carbon diffusion into the Mo bulk, rather than a nucleation layer.

I. Introduction

Molybdenum is a common substrate for diamond thin film growth, since it is a carbide-forming metal under the conditions for CVD diamond growth [1]. It is also a substrate with good nucleation properties [2]. Under the conditions used to grow CVD diamond, molybdenum carbide is present in only one chemical composition, Mo_2C , which is advantageous in interpreting the complex roles of metal and carbide in the nucleation of CVD diamond. We have investigated the "reverse-growth", i.e. dissolution of CVD diamond into the molybdenum substrate, and oxidation of CVD diamond at relatively low pressures and temperatures. Using the photoelectron emission microscope [3,4] (PEEM), both of these processes have been observed in situ. The resulting surface morphologies may be placed in one-to-one correspondence with the sites previously occupied by CVD diamond crystallites.

Emission microscopy is a high contrast method. In the photoelectron emission microscope, variations in the photoelectron yield from the substrate is the source of contrast and image intensity. If the surface has a work function less than the illumination energy, there will be some ejected photoelectrons to form an image. When the work function is greater than the illumination energy, there will be no photo-

electron emission, and hence no intensity in the image. In our experiment, the illumination energy is about 5.1 eV, so that the clean molybdenum surface is relatively dark in the image, but the carbon covered surface, and diamond, is bright.

With photoelectron emission microscopy, CVD diamond [5,6], oxygen adsorption and carbon deposition [7] are all easily observed on molybdenum, due to strong variations in photoelectron yield upon adsorption/desorption of carbon or oxygen. The PEEM method has been used in several studies of carbon and carbide layers on Mo [8-10].

Using thermal gravimetric analysis, at least two groups, C.E. Johnson et al.[11] and R. R. Nimmagadda et al.[12], have studied the oxidation behavior of CVD diamond films in the temperature ranges of 900 to 1050 K and 800 to 1050 K respectively. Both groups found that CVD diamonds start to oxidize appreciably at 950 K, although the oxidation rate of CVD diamonds was found to depend on the concentration of methane used in the preparation of the diamond films.

Most recently, Bachmann et al. [13] have studied the post-growth etching of continuous polycrystalline CVD diamond films. These studies have been mainly concerned with the oxidative attack of carbon impurities in inclusions and grain boundaries of the diamond films. The oxidation was performed at atmospheric pressure in pure oxygen at 875 K.

The amount of diamond and SiC residue left after polishing Mo substrates and heat treatment is the object of a study by Lux

and co-workers [14]. Using imaging SIMS, they showed that diamond could be dissolved into the molybdenum surface. Spectral analysis showed the removal of diamond, and formation of carbide, but the image resolution was not sufficient to examine the post-etching surface morphology.

II. Experimental

The CVD diamond samples under examination were deposited on polycrystalline molybdenum substrates [15] using the hot filament assisted CVD technique [16]. All of the substrates were polished using diamond paste and ultrasonically cleaned in alcohol before deposition. Typical growth conditions were: 1% methane in hydrogen feed gas, 60 sccm gas flow, 50 torr growth pressure, and 1175 to 1225 K substrate temperature. The samples were mounted on a ceramic holder which could be detached from the fixed holder socket in the growth chamber and transferred to the measurement chamber. Details of the transfer system can be found in ref. [17]. The growth time ranged from 20 to 90 minutes. The nucleation of CVD diamond was controlled so that only discontinuous diamond films were formed. Unless otherwise specified, all samples were transferred to the measurement chamber after growth was completed and the samples were allowed to cool, without exposure to air.

Heating of the CVD diamond samples was carried out by electron bombardment. The temperature of the sample was measured

with a two color pyrometer [18]. For experiments on oxidation, the oxygen was introduced into the vacuum chamber through a variable leak valve located at the bottom of the chamber. All of the experiments were observed in real-time using the PEEM. The processes were recorded on either video tape or 35mm film.

For the X-ray photoelectron spectra (XPS) reported below, the standards for Mo, diamond and Molybdenum carbide are: a 99.999% pure Mo (100) single crystal, a thick CVD diamond film and a Mo substrate which has been exposed to the diamond deposition environment for two hours at 1375 K. The presence of diamond and molybdenum carbide on the substrates was confirmed by x-ray diffraction.

The vacuum chamber and PEEM are described in refs. [5] and [19]. An accelerating field between the sample and second lens element is the basis of image formation in emission microscopy. In our microscope 10 kV are applied between the electrically grounded sample and the PEEM at a 4 mm working distance.

III. Results

A. Dissolution in Vacuum

For the conditions used in these experiments, there was no observable diamond dissolution into Mo below 1400 K. Figure 1a is a scanning electron microscope (SEM) image of a typical CVD diamond film. Upon heating to 1470 - 1500 K, dissolution could be detected by direct observation, at 1500 K the central area of the specimen was flat and smooth. Due to uneven heating, the center

of the specimen reached the maximum temperature, and was devoid of diamond particles, but the edges were less affected, and an intermediate area of c. 100 μm width showed some half-dissolved diamond crystallites. Figure 1b shows an ex situ SEM image of such a region.

The SEM images reveal details on the morphology of the diamond crystallites and the substrate near the diamond sites. Evidence of dissolution can be clearly seen. In addition, what appear to be grain boundaries are visible, and raised, rounded features that are similar to morphologies due to melting. For reasons detailed below, the material next to the diamond residue is probably composed entirely of Mo-carbide.

X-ray photoelectron spectroscopy was used to characterize the samples before and after the heating. Before heating, the XPS peak for diamond (C 1s) was observed at 283.6 eV (binding energy), and the Mo 3d_{5/2} at 227.3 eV. The dissolution of diamond into the substrate resulted in a new peak at 282.3 eV assigned to the C 1s level in Mo₂C [20], but no shift in the Mo peak. The carbide was identified by x-ray diffraction to be α -Mo₂C [21,22]. These XPS spectra are not reliable quantitative measures of diamond-to-carbide conversion, because the sampled area almost always includes substrate-edge regions where the heating is uneven, and therefore the conversion of diamond to carbide is incomplete.

In order to observe the diamond dissolution more efficiently, a sparsely nucleated substrate was prepared. The

molybdenum surface was first covered with a "normal" deposition lasting 20 minutes. Small ($\ll 1 \mu\text{m}$ dia.) diamonds, with a nucleation density of c. $10^5/\text{cm}^2$ were observed on the surface. The substrate was heated during PEEM observation in order to dissolve most of these small crystallites. The resulting thin Mo-carbide layer effectively inhibited new nucleation of diamond during a second, 65 minute long deposition. Where some surviving diamonds from the first deposition served as "seeds", growth of diamonds of approximately 1 - 2 μm diameter was observed.

"Seed survival" nucleation is indicated by the location of the second growth diamonds: the center of the substrate, which reaches the highest temperature, is composed entirely of smooth Mo-carbide, and does not nucleate diamond. The images of CVD diamond in figure 2a are from the surrounding region where small seed crystallites survived heating. The images of the diamonds are very bright against the relatively dark substrate surface, in part due to field emission from the diamond crystallites [6].

Figures 2b and 2c are in situ PEEM micrographs ($T = 1500 \text{ K}$) showing the result of the heating of the CVD diamond on the Mo/Mo-carbide substrate. The presence of the crystallites can be determined by the shadows they cast due to the glancing incidence of the u.v. light. The reduction in the size of the crystallites could be seen in (b) and (c). After they disappeared, the substrate was found to have bumps or craters (with central indentations) of about $10 \mu\text{m}$ in diameter left at the diamond sites (See figure 3).

B. Oxidation

Two PEEM micrographs showing the oxidation of a CVD diamond sample are shown in figure 4a and b. A sparsely nucleated CVD diamond sample was chosen because the reduction in the size of the diamond particles could be simply observed.

The chamber pressure was in the mid 10^{-9} Torr range before the sample was heated and the oxygen was introduced. After the sample was heated, the pressure rose to the low 10^{-8} Torr range. Oxygen was introduced into the chamber while the sample was at elevated temperature, resulting in a final pressure of 1×10^{-7} Torr. Some diamonds, on an oxygen covered Mo substrate at 875 K, are shown in fig. 4a. The substrate is dark due to oxygen adsorption. The reduction in the diameter of the diamond crystallites could soon be noticed, and observed continuously until the diamonds were completely gone, fig. 4b, (about one hour).

After the diamonds were completely removed by oxidation, features such as are shown in fig. 4b were found at the diamond sites. The direction of shadows in the PEEM image indicate that these features are pits or depressions in the substrate.

Observation of these substrates with ex situ SEM confirmed the presence of pits at the former diamond sites. Fig. 5a and 5b show two SEM micrographs of the same area on a CVD diamond sample before and after oxidation. It is significant to our interpretation that "pits" in the substrate at diamond sites are observed after a single growth, as in these SEM micrographs, and

for a substrate that has been heated after the first growth, and diamond grown on the seeded surface such as in the process shown in figure 2a-c.

IV. Discussion

The very noticeable changes observed in situ at the diamond sites are the pits left after oxidation and the bumps left after dissolution. The pits left at the diamond sites indicate two things: there is little etching of the carbide layer by oxygen at 875 K, and, the diamonds were partially buried in the carbide layer. The bumps left at the diamond sites after dissolution indicate that there is molybdenum diffusion from the bulk substrate to the surface where the Mo reacts with the CVD diamonds to form Mo-carbide.

While not quantitative, the reduction of the C 1s peak at 283.6 eV after oxidation indicates removal of diamonds from the substrate surface. The C 1s peak at 282.3 eV in the spectra after oxidation indicates that the carbon in the form of carbide with the substrate was not removed by oxidation. Similarly, when diamond crystallites are heated in vacuum on Mo substrates, the conversion of diamond carbon (283.6 eV) to carbide (282.3 eV) indicates that carbide forms at the expense of diamond carbon. The lack of CVD diamond nucleation on pure Mo-carbide [23] or Mo-carbide substrates produced by diamond dissolution indicates that the carbide layer is an effective nucleation inhibitor.

We conclude that when CVD diamond deposition is started,

diamond nucleation and carbide formation are simultaneous, or at the very least, if carbide formation precedes diamond growth, nucleation takes place on areas of the substrate still free of carbide. Carbide grows as long as the carbon supply continues and mass transport of Mo through the carbide layer to the carbon-rich surface is possible; growth of the carbide layer continues until a limiting thickness is reached. Because the carbide grows with the diamond, part of the diamond crystallite is buried in the carbide layer. When the diamond crystallite is removed by oxidation, a crater is left on the diamond site.

Because the carbide layer under the diamond crystallite is thin, mass transport of Mo is possible through the base of the carbide crater surrounding the diamond. During diamond dissolution, a "bump" is left at the diamond site as a result of molybdenum transport through the cavity in the carbide layer, which reacts with the diamond carbon to form a "plug" at the diamond site.

A carbide layer is always found between a carbide forming substrate and the CVD diamond film grown on it. It is therefore assumed by many that the carbide layer is the cause of CVD diamond nucleation [23,24]. The observations made using in situ PEEM and SEM of CVD diamond oxidation and dissolution suggest that the carbide layer and CVD diamond are not directly related by a "cause and effect" relationship during diamond deposition. In fact, the growth of carbide can alter the substrate morphology to such a degree that nucleation of CVD diamond on a carbide layer

is impossible.

A schematic diagram of the growth of CVD diamond on molybdenum, summarizing the information obtained from PEEM and SEM observation is shown in figure 5. Initial growth of diamond and the Mo-carbide layer is shown, with no secondary nucleation on the carbide. The diamonds are embedded in the Mo-carbide film. Oxidation of the diamond leaves a "pit" in the Mo-carbide. Heating the diamond in vacuum allows Mo from beneath the Mo-carbide layer to move through the thin base of the "pit", where it reacts with the diamond carbon to form a Mo-carbide "plug" or crater-like bump on the surface. The shape of the bump indicates that the Mo is mobile, since it wells up into the pit. There is some transport along the surface on the carbide layer, since the bumps seem to flow. It is clear from the shape of the "pit" that the diamond-carbide interface is stable, but the carbon-metal interface is reactive, until metal transport ceases. The carbide layer is a diffusion barrier, both for diamond carbon into the Mo, and, to a lesser extent, for Mo. The morphology of the bumps left at the diamond sites indicates that Mo transport is the limiting factor in the reaction of diamond with the Mo substrate at the temperatures used in this study.

Preliminary experiments show that pure Mo-carbide polished with diamond paste or SiC sandpaper show excellent CVD diamond nucleation. It is possible that the Mo-carbide layer protects the seeds left after polishing by inhibiting loss of the seeds to Mo-carbide formation at standard growth temperatures.

V. Summary

The Oxidation and dissolution of CVD diamond has been studied using PEEM, XPS and SEM. Real-time observation of these processes was performed using photoelectron emission microscopy. After diamond particles were removed by oxidation, pits were observed at the diamond sites. The pits left at the diamond sites indicate that the carbide layer found on diamond substrates grows simultaneously with diamond. CVD diamond was found to dissolve into the Mo substrate when the temperature was raised above 1455 K. Dissolution of diamond particles was observed with both PEEM (real-time) and SEM (ex-situ). The formation of "bumps" or "plugged craters" strongly indicates that it is the molybdenum from the substrate that is the mobile species in carbide formation, and therefore the carbide layer must be a barrier to both carbon and molybdenum diffusion. XPS showed only Mo_2C was left after diamonds were removed by oxidation or by heating.

Acknowledgements

This work was supported by the Office of Naval Research through SDIO/IST grant N00014-91-J-1596. Financial support was also received from the CMSS program of Ohio University and NATO. AT&T Bell Laboratories are gratefully acknowledged for the SEM micrographs in figure 1a and b.

References:

1. P.O. Joffreau, R. Haubner, and B. Lux, J. Ref. Met. -Hard Mat., 7 (1988), 186.
2. B. Lux and R. Haubner, in "Diamond and Diamond-Like films and Coatings", R.E. Clausing, ed., Plenum Press, New York, 1991, p 579.
3. R.A. Schwarzer, Microscopica Acta 84 (1981) 51.
4. O. H. Griffith and G. F. Rempfer, in Advances in Optical and Electron Microscopy, 10, eds. R. Barer and V.E. Cosslett (Academic Press, London, 1987, p 269.
5. C. Wang and M.E. Kordesch, Ultramicroscopy 36 (1991) 154.
6. C. Wang, A. Garcia, D.C. Ingram, M. Lake and M.E. Kordesch, Electronics Letters 27 (1991) 1459-1461.
7. A. Garcia, C. Wang and M.E. Kordesch, Appl. Phys. Lett. 61 (1992) 2984.
8. M.E. Kordesch, Proceedings of the 3rd International Symposium on Diamond and Diamond Materials, The Electrochemical Society, Pennington, NJ, 1993, in press.
9. W. Engel, PhD Thesis, Free University Berlin, 1968.
10. M. Mundschau, E. Bauer and W. Sweich, Catal. Lett. 1 (1988) 405.
11. C.E. Johnson, M.A.S. Hasting, and W.A. Weimer, J. Mater. Res., 5 (1990) 2320.
12. R.Rao, Nimmadadda, A. Joshi, and W.L. Hsu, J. Mater. Res., 5 (1990) 2445.

13. P.K. Bachmann, D. Leers, and D.U. Weichert, *Diamond Relat. Mater.* 2 (1993) 683.
14. R. Steiner, G. Stingeder, M. Grasserbauer R. Haubner and B. Lux, *Diamond. Relat. Mater.* 2 (1993) 958.
15. A.D. Mackay, Inc., New York, NY. 99.95% Mo, 0.25 mm thick.
16. B.V. Derjagin, D.V. Fedoseev, V.M. Lukyanovich, B.V. Spitzin, V.A. Ryabov, and A.V. Lavrentyev, *J. Cryst. Growth* 2 (1968) 380.
17. A. Garcia and M. E. Kordesch, *J. Vac. Sci. Technol.*, A11 (1993) 461.
18. Mikron Instrument Co., M77, Wyckoff, NJ 07481.
19. W. Engel, M.E. Kordesch, H.H. Rotermond *Ultramicroscopy* 36 (1991).
20. C. Wang, Ph.D. Dissertation, Ohio University 1993. UMI Dissertation Services, No.: 9322371, 1993.
21. Powder Diffraction File, International Centre for Diffraction Data, Swarthmore PA 19081 - 2389, 1989.
22. E. K. Storms, "The Refractory Carbides", Academic Press, New York, 1967, p 127.
23. See ref 1, figure 9.
24. B.R. Stoner, G.-H. M. Ma, S.D. Wolter, and J.T. Glass, *Phys Rev. B*, 45 (1992) 11,067.

Figure Captions:

Figure 1: a) SEM micrograph of a typical hot filament CVD diamond film grown in our system. A JEOL 6300F was used.

b) SEM image of diamond dissolved into Mo. The sample temperature at this exact spot is unknown. Maximum temperature at center, where no diamond survived: $T = 1500$ K.

Figure 2: a) PEEM micrograph of individual CVD diamonds on a Mo/Mo-carbide substrate at 300 K. The diamonds are bright spots, due to field emission from the crystallites. The substrate is dark compared to the CVD diamonds.

Bar = 50 μm .

b) Same as a) showing partial dissolution of diamond, $T = 1500$ K. Note the illumination shadows in the figure. The relative contrast between the crystallites and the substrate is less than in a) due to thermionic electron emission from the substrate. Bar = 50 μm .

c) Same as b), all diamonds dissolved. "Bumps", indicating Mo transport to the diamond site, and little diffusion parallel to the surface, are clearly observed at the former diamond sites. Bar = 50 μm .

Figure 3.: PEEM micrograph of "bumps". Note depressions in center of some of the bumps. Bar = 30 μm .

Figure 4. a) In situ PEEM image of diamonds during oxidation. The substrate is dark due to oxygen adsorption, which raises the work function of the surface beyond the photoelectron emission threshold. The CVD diamonds are bright spots in the image. Bar = 50 μm .

b) In situ PEEM, showing "pits" at former diamond sites. Bar = 50 μm .

Figure 5. a) SEM image of CVD diamonds on Mo. A JEOL -5300 SEM was used.

b) The same area after oxidation. Pits at the sites formerly occupied by diamond crystallites are clearly evident. The pits are present even for "first growth" diamond deposition. No preheating or diamond pre-dissolution was performed on this sample.

Figure 6. Schematic diagram of the morphology and composition of CVD diamond on Mo. Pits remain after diamond oxidation, and "bumps" or crater-like features result during dissolution when Mo reacts with CVD diamond to form Mo-carbide at the diamond site.

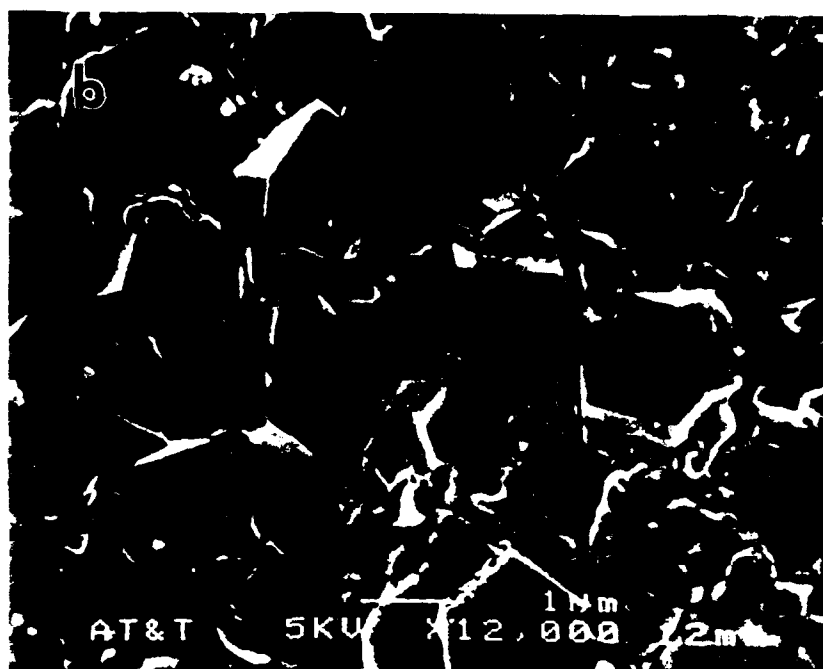


Fig 1

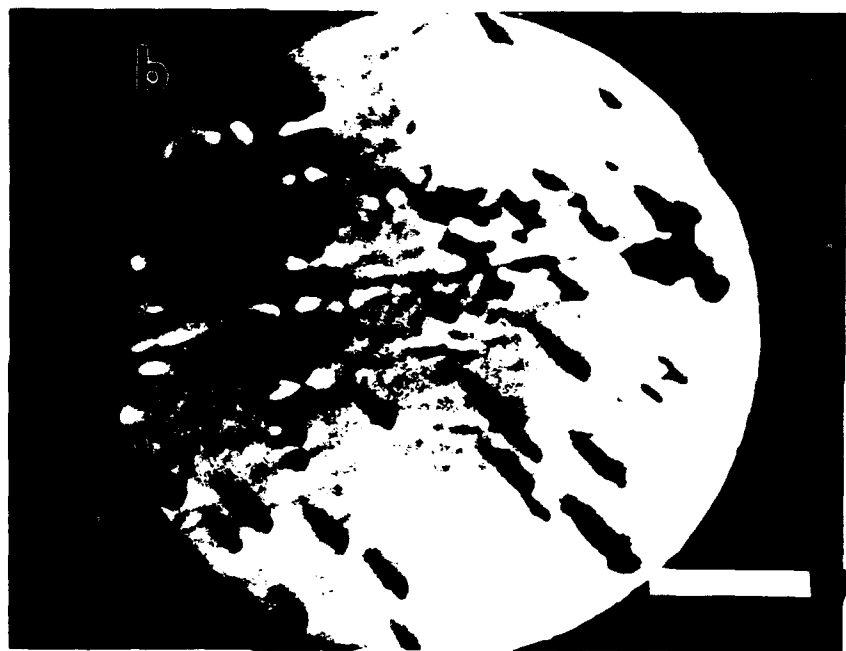


Fig 2



Fig 3

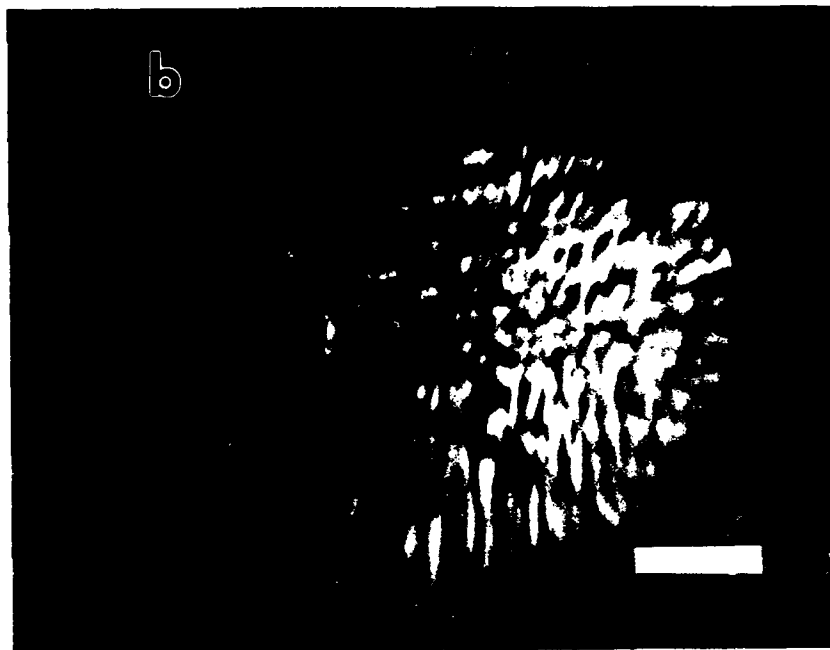
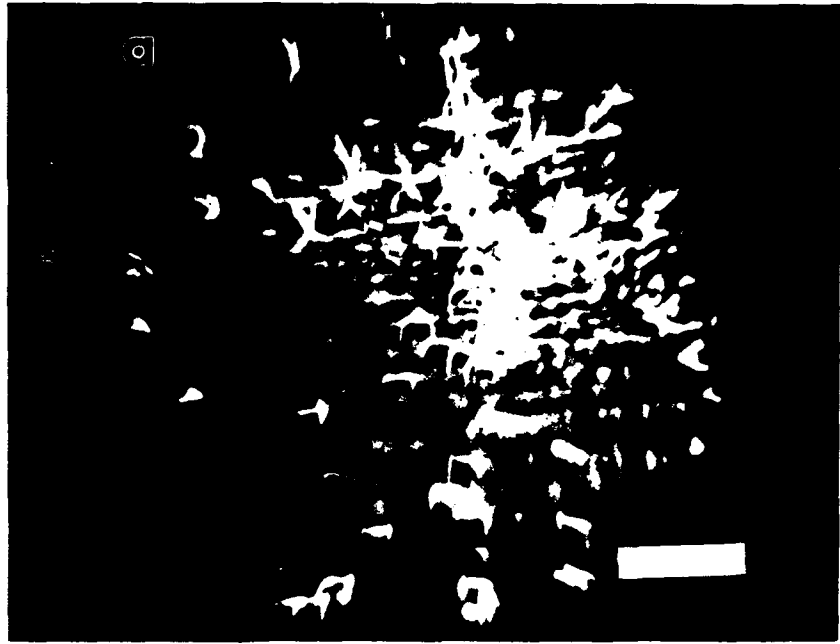


Fig 4

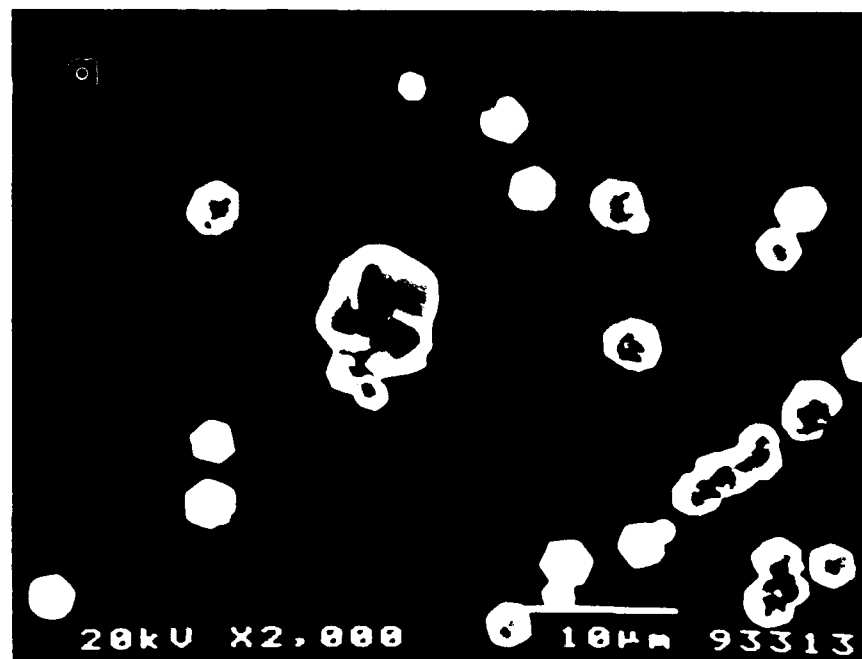
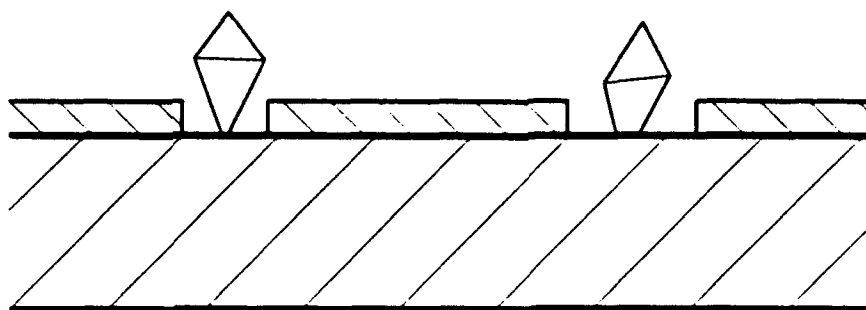
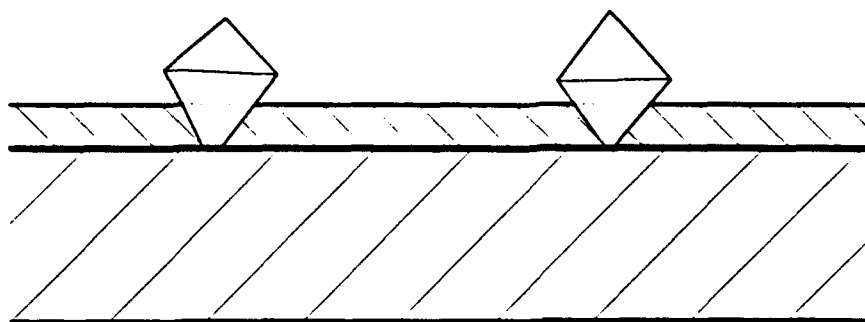


Fig 5

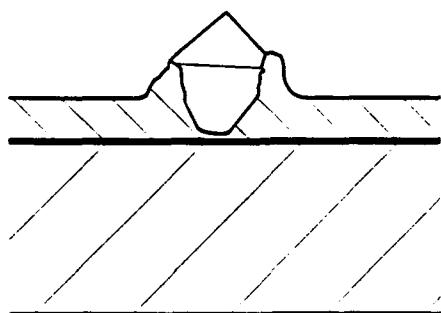


Carbide

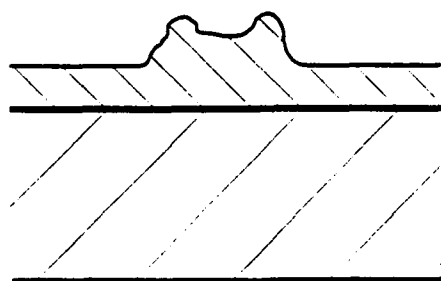
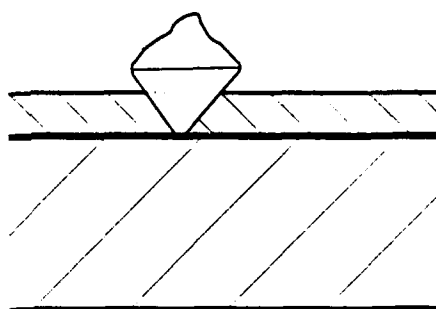
Mo



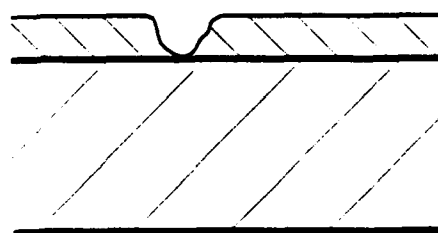
Heating



Oxidation



"Bump\Plug"



"Pit"

Fig
6

Non-Diamond Carbon Removal from the Surface of CVD Diamond Films

W.Engel*, D.C. Ingram, J.C. Keay and M.E. Kordesch

Condensed Matter and Surface Sciences Program

Department of Physics

Ohio University, Athens OH 45701 -2979

***Permanent address: Fritz Haber Institute, Berlin, Germany.**

Thin (10nm) carbon films are found to adhere to Chemical Vapor Deposited (CVD) diamond films. This layer may be removed with a simple wash in isopropanol. The carbon layer is structureless in TEM, and is probably a hydrocarbon residue remaining on the diamond surface after the cessation of the growth process.

The ratio of non-diamond carbon to diamond in CVD diamond thin films has been studied intensively since the discovery of the low temperature-low pressure synthesis of diamond. This ratio has long been the measure of the success of a particular growth method. In this letter we show that some non-diamond carbon residue may be left on the diamond surface after growth, and that this layer can easily be removed with a simple rinse in isopropanol.

Several measurements, most notably micro-Raman spectroscopy, have been used to determine the bulk sp^2/sp^3 carbon ratio [1,2] or the hydrogen content of CVD diamond films. Measurements of hydrogen content and sp^2/sp^3 carbon bond ratios may be influenced by the presence of the carbon layer described below.

Gleason and co-workers have determined the surface to bulk ratio of H incorporated into diamond films using NMR spectroscopy [2-5] and have made quantitative comparisons with NMR and infra-red spectroscopy. Gleason has observed the effects of isopropanol rinsing of CVD diamond in NMR [6], and suggested the isopropanol wash procedure. We present a direct observation of the carbon residue layer and its removal using TEM, and a direct measurement of hydrogen content in as-grown and isopropanol-washed films using RBS/ERS.

The CVD diamond used for the TEM (Philips CM120) study was deposited directly onto a molybdenum TEM grid (Pelco 100/300 Mo double grid) in a HFCVD reactor from 1% methane in hydrogen for 10 - 20 minutes [7].

Figure 1a shows an as-grown diamond, figure 1b shows a diamond that was rinsed with isopropanol by dipping the TEM grid in isopropanol for several seconds.

The overlayer clearly visible on the diamond in figure 1a is greatly reduced by the isopropanol rinse. The carbon layer was observed on 10 - 12 different specimens grown at different temperatures and for different lengths of time, although no systematic analysis of the layer thickness or structure was attempted. The TEM was fitted with a liquid nitrogen cold finger to reduce hydrocarbon contamination from the microscope itself, and the films were not observed to re-appear during examination.

Fallon and Brown [8,9] have also observed a layer on the surface of diamond crystals using high resolution TEM. Through the use of electron energy loss spectroscopy (EELS) they were able to demonstrate that the layer was predominantly sp^2 bonded. The thickness of the layer they observed was similar to ours and was amorphous.

We have also examined a flame deposited diamond film. This film was analyzed using Rutherford Backscattering Spectroscopy (RBS) and Elastic Recoil Spectroscopy (ERS) [10]. The probe used in each case was a beam of 2.50 MeV $^4\text{He}^{++}$ particles. Figure 2, inset, shows the sample-detector geometry used for the RBS and ERS measurements. The sample was tilted so that the beam would be incident at $\phi = 75^\circ$ from the surface normal. The backscattered alpha particles were collected with a detector located at 168° with respect to the incident beam. A second detector located at an angle of 30° from the incident beam simultaneously acquired a hydrogen recoil spectrum. A 13 μm thick Mylar stopper foil was placed in front of this detector to eliminate forward-scattered alpha particles from the spectrum. The recoil spectrum was normalized to the RBS carbon signal and subsequently fitted using

RUMP which is capable of simulating both RBS and ERS spectra [11]. Figure 2 shows the concentration of hydrogen as a function of depth used to fit the ERS data.

RBS and ERS data were acquired from the sample first in the as-received state. The sample was then ultrasonically cleaned in isopropanol for 25 minutes and a second set of RBS and ERS spectra was taken.

The spectrum from the sample in the as-received state has a surface peak of 11.5% atomic percent hydrogen, which then falls off to 5% hydrogen at a depth of ~100 nm. The concentration of hydrogen then continues to fall off at a linear rate to about 2% in the bulk diamond. In the washed state there is almost a 50% reduction in the hydrogen concentration over the entire spectrum relative to that measured on the control sample. The surface hydrogen concentration is 6.5% which then drops to 2% at ~100 nm, and reaches a bulk level similar to that of the sample in the as-received state.

The equal percentage drop in the hydrogen content over the entire spectrum of the washed sample highlights a major problem when taking data from polycrystalline diamond samples. For a smooth surface, the variation of an impurity concentration as a function of energy for both RBS and ERS is indicative of a variation in the impurity concentration as a function of depth. However, for a polycrystalline surface, the possibility exists for an impurity to be on the surface of an individual grain yet appear to be below the surface of the sample as detected by RBS or ERS. In particular, for samples which have gaps between individual grains (see Figure 3), two types of events are possible that shift the detected energy to lower values. One type occurs

when an incident particle recoils an hydrogen atom through the diamond, and the second type occurs when the alpha particle passes through the diamond and then recoils an hydrogen atom upon exiting the crystallite. These surface events will be detected at energies characteristic of subsurface recoils, and thus will artificially increase the apparent subsurface hydrogen concentration. Therefore, the overall reduction in the hydrogen level observed in the figure 2 data is more likely to be due to hydrogen being removed from the surface of individual diamond crystals rather than by the isopropanol penetrating the crystals and removing the hydrogen from their bulk.

In summary, we have shown that a hydrogen bearing layer of amorphous carbon can exist on the surface of diamond. This layer is not particularly tenacious as it can be removed by an isopropanol rinse. The importance of this layer to studies involving Raman spectroscopy is clear since the scattering cross-section from sp^2 carbon compared to sp^3 is known to be fifty times greater [12].

Acknowledgements: This work was supported by the Office of Naval Research and SDIO/IST through grant No. N 00014 - J 1596 and a cooperative research grant from NATO. We thank Christoph Boettcher for the TEM micrographs, and the Fritz Haber Institute for the use of their facilities. C. Wang prepared the CVD diamonds for TEM. The flame deposited CVD diamond film used in RBS and ERS was provided by K. Gleason.

References:

1. M. Silveira, M. Becucci and E. Castellucci, *Diamond and Rel. Mater.*, 2 (1993) 1257.
2. K.M. McNamara, K.K. Gleason, D.J. Vestyck and J.E. Butler, *Diamond and Rel. Mater.*, 1 (1992) 1145.
3. S. Mitra and K.K. Gleason, *Diamond and Rel. Mater.*, 2 (1993) 126.
4. K.M. McNamara, K.K. Gleason and C.J. Robinson, *J. Vac. Sci. Technol.*, 10 (1992) 3143.
5. K.M. McNamara, D.H. Levy, K.K. Gleason and C.J. Robinson, *Appl. Phys. Lett.* 60 (1992) 580.
6. K.K. Gleason, Private Communication
7. C. Wang, Ph.D. Thesis Ohio University 1993, "A Photoemission Electron Microscope Investigation of CVD Diamond Films and Diamond Nucleation", UMI Dissertation Services, Ann Arbor, MI, No. 9322371.
8. P.J. Fallon and L.M. Brown, *Electron Microscopy, Vol. 1 EUREM 92*, Granada, Spain (1992) 257.
9. P.J. Fallon and L.M. Brown, *Diamond and Rel. Mater.*, 2 (1993) 1004.
10. D.C. Ingram, A.W. McCormick and P.P. Pronko, *Nucl. Instr. and Meth.*, B6 (1985) 430.
11. L.R. Doolittle, *Nucl. Inst. and Meths.* B9 1985 334
12. N. Wada, P.J. Gaczi, S.A. Solin, *J. Non-Cryst. Solids* 35/36 1980 543

Figure Captions:

Figure 1.: a) TEM micrograph of a hot filament CVD diamond crystallite grown on a Mo TEM grid. Beam voltage 120 kV. The bar is 30 nm.

b) a micrograph from the same TEM grid, after a gentle rinse in isopropanol. Bar is 20 nm.

Figure 2.: inset: RBS and ERS scattering/recoil geometry. top: Atomic hydrogen concentration derived from RBS/ERS spectra of the as-received flame deposited CVD diamond film. bottom: same as top, after 25 min. ultrasonic cleaning in isopropanol.

Figure 3.: SEM micrograph of the flame-deposited CVD diamond sample.

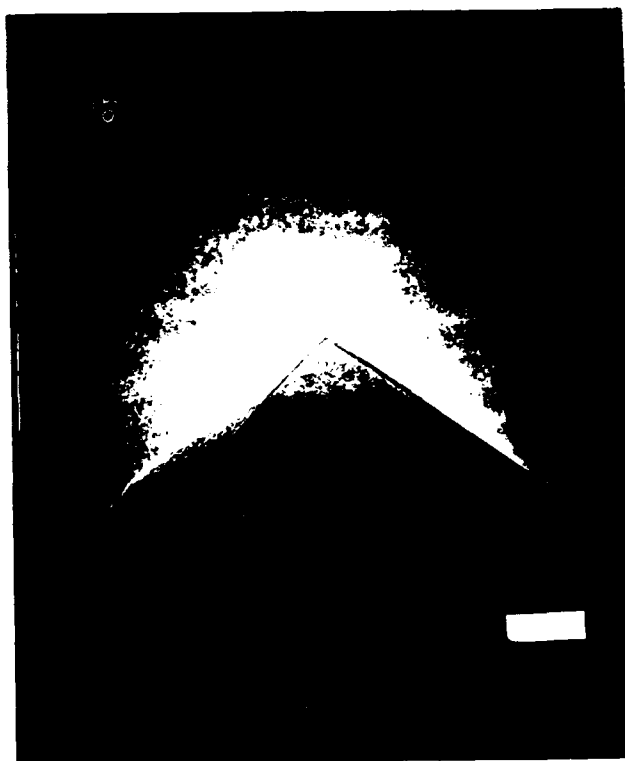
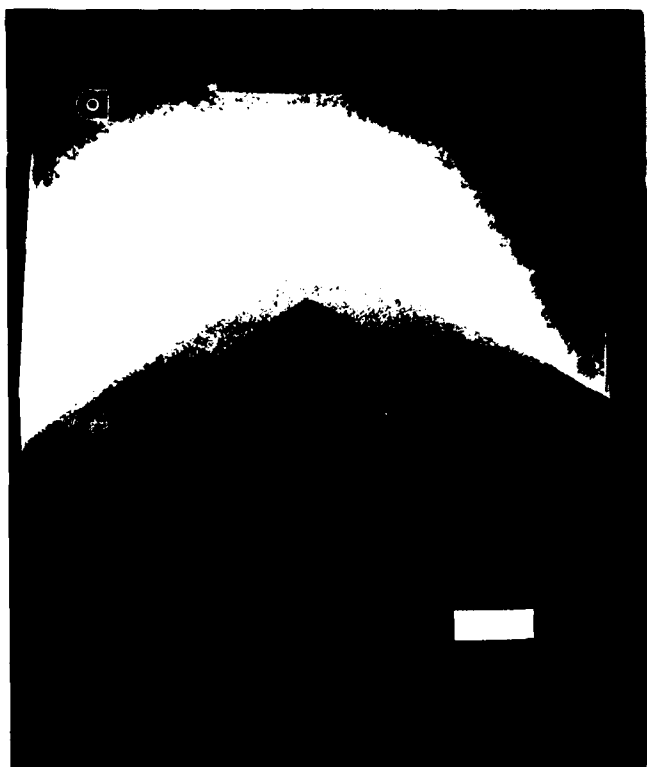


Figure 1 a + b

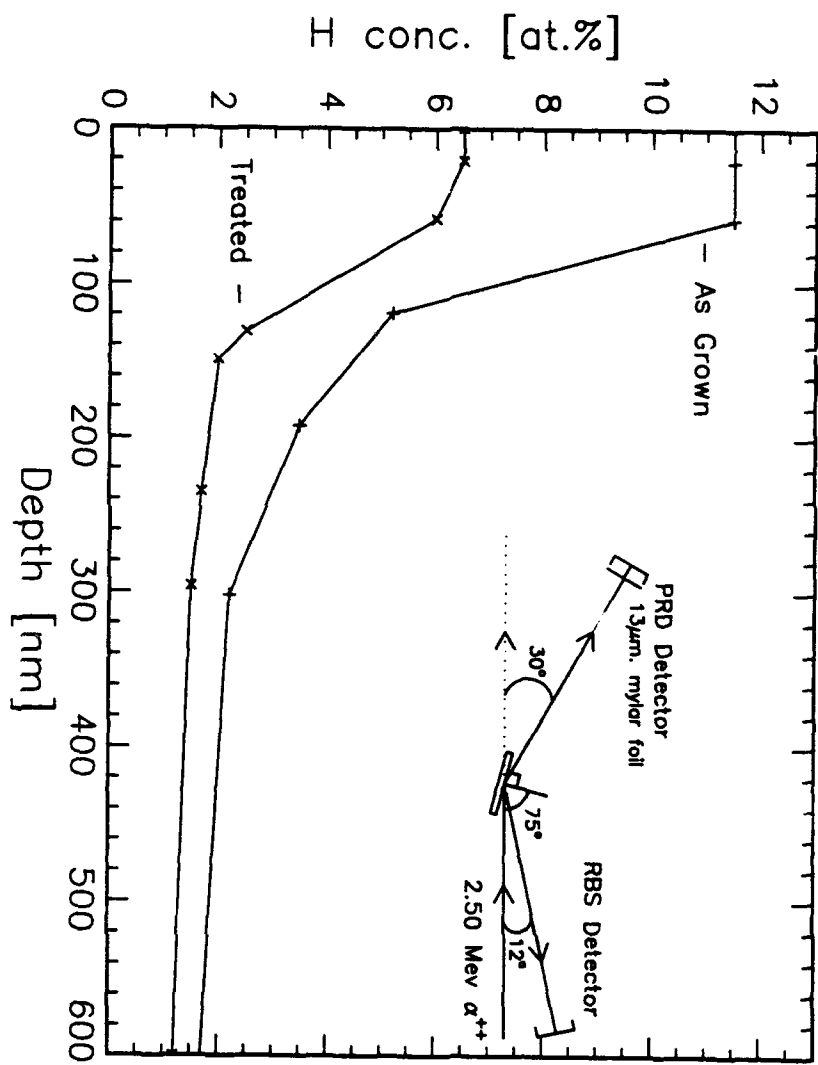




Figure 3